Available online at www.sciencedirect.com

SciVerse ScienceDirect

Ceramics International 39 (2013) 7285–7289

CERAMICS INTERNATIONAL

www.elsevier.com/locate/ceramint

Short communication

Simultaneous synthesis and consolidation of $Mg_4Al_2Ti_9O_{25}$ by pulsed current activated heating and its mechanical properties

In-Jin Shon[a,*], Song-Lee Du[a], Jung-Mann Doh[b], Jin-Kook Yoon[b]

[a]*Division of Advanced Materials Engineering and the Research Center of Advanced Materials Development, Engineering College, Chonbuk National University, Jeonbuk 561-756, Republic of Korea*

[b]*Interface Control Research Center, Korea Institute of Science and Technology, PO Box 131, Cheongryang, Seoul 130–650, Republic of Korea*

Received 7 January 2013; received in revised form 17 February 2013; accepted 18 February 2013
Available online 26 February 2013

Abstract

The simultaneous synthesis and densification of nanostructured $Mg_4Al_2Ti_9O_{25}$ from $4MgO–Al_2O_3–9TiO_2$ powders by a pulsed current activated sintering was investigated. The advantage of this process is that it allows for very quick densification to occur near the theoretical density and inhibits grain growth. A highly dense nanostructured $Mg_4Al_2Ti_9O_{25}$ compound was produced with the simultaneous application of 80-MPa pressure and a pulsed current within 1 min. The sintering behavior, grain size and mechanical properties of $Mg_4Al_2Ti_9O_{25}$ were investigated.

Keywords: C. Mechanical properties; Compound; Microstructure; Nanostuctures

1. Introduction

A wet chemical method has been developed for the preparation of $Mg_4Al_2Ti_9O_{25}$ ceramics by the gel-carbonate method [1,2]. High-purity $Al(NO_3)\cdot 2H_2O$ was dissolved in distilled water and the solution was mixed with $TiOCl_2$. Mixed gels of the hydrated titania $TiO_2\cdot xH_2O$ ($90 < x < 120$) and alumina $Al_2O_3\cdot yH_2O$ ($80 < y < 110$) were precipitated by adding the combined solution to 1 M ammonium carbonate at around 30 °C. The $Mg_4Al_2Ti_9O_{25}$ compound is a potential candidate for microwave antenna substrate in communication systems, because of its high dielectric constant and low dielectric losses [2]. However, as in the case of many such compounds, there is concern related to low fracture toughness below the ductile–brittle transition temperature. The addition of a second phase to form composites and nanostructures is a common approach to improve the mechanical properties. Nanocrystalline materials have received much attention as advanced engineering materials with improved physical and mechanical properties [3,4]. Attention has been directed to the application of nanomaterials as they possess high strength, high hardness, and excellent ductility and toughness [5,6]. Recently, nanocrystalline powders have been developed using thermochemical and thermomechanical processes such as the spray conversion process (SCP), co-precipitation and high-energy milling [7–9]. However, grain sizes in sintered materials are greater than those in pre-sintered powders due to fast grain growth during the conventional sintering process. Therefore, even though the initial particle size is less than 100 nm, the grain size increases rapidly up to 2 μm or greater during conventional sintering [10]. As a result, controlling the grain growth during sintering is one of the keys to the commercial success of nanostructured materials. Pulsed-current-activated sintering (PCAS), which can produce dense materials within 2 min, has been shown to be effective for achieving this goal [11,12].

In this study, a method for the simultaneous synthesis and consolidation of the $Mg_4Al_2Ti_9O_{25}$ compound is investigated using the PCAS method. The goal of this research is to produce a dense nanostructured $Mg_4Al_2Ti_9O_{25}$ compound in one step. In addition, the mechanical properties and

*Corresponding author. Tel.: +82 63 270 2381; fax: +82 63 270 2386.
E-mail address: ijshon@chonbuk.ac.kr (I.-J. Shon).

0272-8842/$ - see front matter © 2012 Elsevier Ltd and Techna Group S.r.l. All rights reserved.
http://dx.doi.org/10.1016/j.ceramint.2013.02.052

microstructure of the $Mg_4Al_2Ti_9O_{25}$ compound were also studied.

2. Experimental procedure

MgO powder with a grain size of <1 μm and 99% purity, Al_2O_3 powder with a grain size of <2.2 μm and 99.99% purity and TiO_2 powder with a grain size of <45 μm and 99.8% purity were supplied by Alfa. The powders (Al_2O_3–4MgO–9TiO_2) were first milled in a high-energy ball mill (Pulverisette-5 planetary mill) at 250 rpm for 10 h. Tungsten carbide balls (9 mm in diameter) were used in a sealed cylindrical stainless-steel vial with an argon atmosphere at a ball-to-powder weight ratio of 30:1.

The powders were placed in a graphite die (outer diameter: 35 mm; inner diameter: 10 mm; height: 40 mm) and introduced into a PCAS apparatus, which is shown schematically in Ref. [11,12]. The PCAS apparatus included a 30-kW power supply, which provided a pulsed current (on time: 20 μs; off time: 10 μs), and a 50-kN uniaxial press. The system was first evacuated and a uniaxial pressure of 80 MPa was applied. A pulsed current was then activated and maintained until the densification rate was negligible, as indicated by the real-time output of the shrinkage of the sample. The shrinkage was measured by a linear gauge which detected the vertical displacement. Temperatures were measured using a pyrometer focused on the surface of the graphite die. Upon the completion of the process, the induced current was turned off and the sample was cooled to room temperature. The process was performed under vacuum at 5.33 Pa.

Microstructural information was obtained from product samples that had been polished and thermally etched for 1 h at 1050 °C. Compositional and microstructural analyses of the products were conducted through X-ray diffraction (XRD) and field emission scanning electron microscopy (FE-SEM) with energy dispersive spectroscopy (EDS). Vickers hardness measurements were performed on polished sections of the $Mg_4Al_2TiO_{25}$ compound using a 5-kg load and a 15-s dwell time.

The grain sizes of the powders and sintered product were calculated from the full width at half-maximum (FWHM) of the diffraction peak using Suryanarayana and Norton's formula [13]

$$B_r(B_{crystalline}+B_{strain})\cos\theta = k\lambda/L+\eta\sin\theta \quad (1)$$

where B_r is the full width at half-maximum (FWHM) of the diffraction peak after instrumental correction; $B_{crystalline}$ and B_{strain} are the FWHMs caused by small grain size and internal stress, respectively; k is a constant (with a value of 0.9); λ is the wavelength of the X-ray radiation; L and η are the grain size and internal strain, respectively; and θ is the Bragg angle. The parameters B and B_r follow Cauchy's form with the relationship: $B=B_r+B_s$, where B and B_s are the FWHMs of the broadened Bragg peaks and the standard sample's Bragg peaks, respectively.

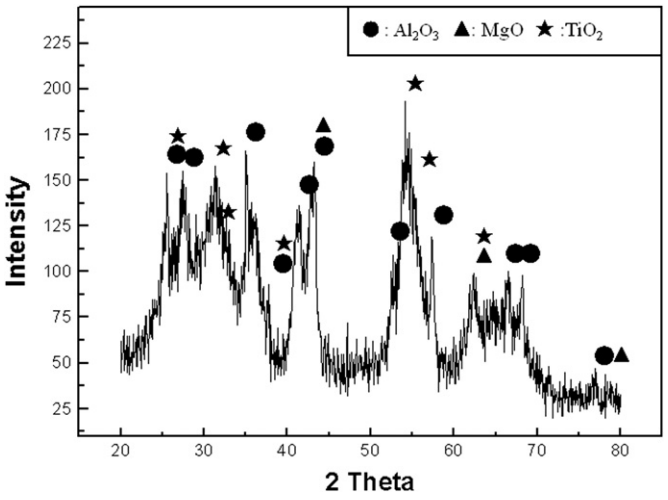

Fig. 1. X-ray diffraction pattern of the powders of Al_2O_3, MgO and TiO_2 milled for 10 h.

3. Results and discussion

Fig. 1 demonstrates the X-ray diffraction pattern of the 4MgO–Al_2O_3–9TiO_2 powders after high-energy ball milling for 10 h. Only MgO, TiO_2 and Al_2O_3 peaks were detected. Fig. 2 shows a plot of $B_r\cos\theta$ versus $\sin\theta$ of MgO, TiO_2 and Al_2O_3 milled for 10 h, to calculate the particle sizes from XRD data. The average grain sizes of the milled MgO, TiO_2, and Al_2O_3 powders determined by Suryanarayana and Norton's formula were approximately 8, 94 and 16 nm, respectively. The FE-SEM images of 4MgO–Al_2O_3–9TiO_2 powders after milling for 10 h are shown in Fig. 3. The Al_2O_3, TiO_2 and MgO powders were round nanograins with milling and agglomeration. The variations in shrinkage displacement and temperature with heating time during the sintering of the high-energy ball-milled 4MgO–Al_2O_3–9TiO_2 powders under a pressure of 80 MPa are shown in Fig. 4. The application of the pulsed current resulted in shrinkage due to consolidation. As the pulsed current was applied, the shrinkage displacement was nearly constant until 700 °C. Then the shrinkage abruptly increased once above this temperature. The longer the pulsed current corresponded, the more the specimen shrunk. High-energy ball milling treatment allows for the control of compound formation through the fixation of the Al_2O_3, TiO_2, and MgO powder microstructures. Indeed, high-energy ball milling produced finer crystallites, strains and defects. Therefore, the consolidation temperature decreased due to milling because the driving force for sintering and the powder contact points for atomic diffusion increased. Fig. 5 displays the XRD pattern of a specimen sintered from the high-energy ball-milled 4MgO–Al_2O_3–9TiO_2 powders. Only $Mg_4Al_2TiO_{25}$ peaks are detected. According to the X-ray data (Fig. 1 and 5) the interaction between these phases, i.e.,

$$Al_2O_3+4MgO+9TiO_2 \rightarrow Mg_4Al_2TiO_{25} \quad (2)$$

is thermodynamically feasible. FE-SEM images of the

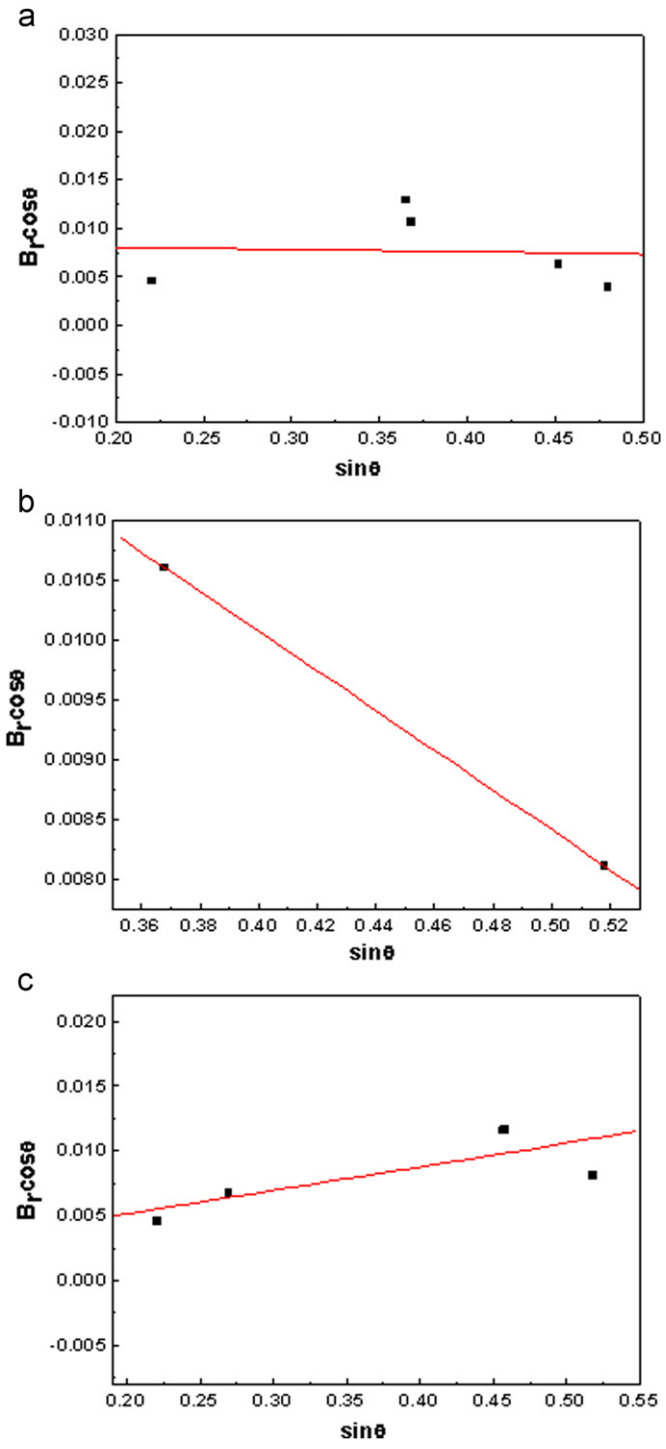

Fig. 2. Plot of B_r ($B_{crystalline}+B_{strain}$)cos θ versus sin θ for Al_2O_3 (a), MgO (b) and TiO_2 (c) powder milled for 10 h.

$Mg_4Al_2TiO_{25}$ compound sintered from $Al_2O_3+4MgO+9TiO_2$ powders milled for 10 h are shown in Fig. 5. A plot of B_r ($B_{crystalline}+B_{strain}$)cos θ versus sin θ of $Mg_4Al_2TiO_{25}$ in Suryanarayana and Norton's formula [13] is shown in Fig. 6. The average grain size of the $Mg_4Al_2TiO_{25}$ calculated from the XRD data using Suryanarayana and Norton's formula was about 170 nm. Thus, the average grain size of the sintered $Mg_4Al_2TiO_{25}$ is not significantly

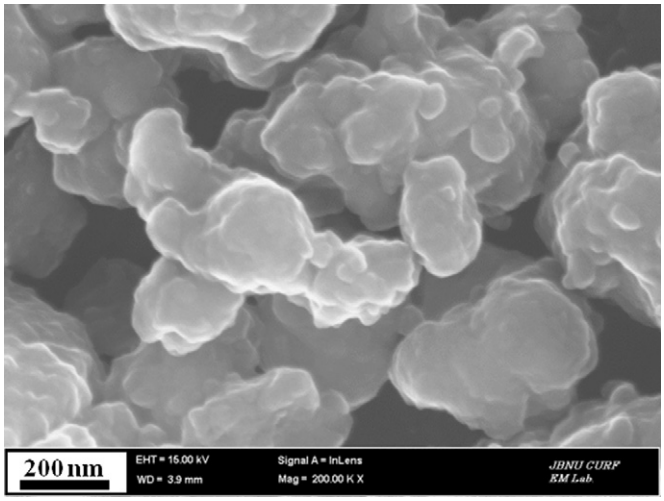

Fig. 3. FE-SEM images of the powders of Al_2O_3, MgO and TiO_2 milled for 10 h.

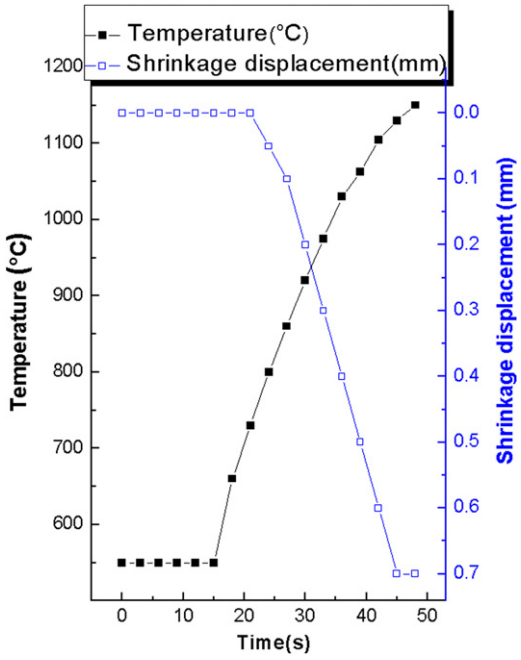

Fig. 4. Variations in temperature and shrinkage with heating time during the sintering of $Al_2O_3+4MgO+9TiO_2$ powders milled for 10 h.

larger than that of the initial powder, indicating the absence of much grain growth during sintering. This retention of the grain size is attributed to the high heating rate and the relatively short-term exposure of the powders to the high temperature. A FE-SEM image of $Mg_4Al_2TiO_{25}$ sintered from $Al_2O_3+4MgO+9TiO_2$ powders milled for 10 h is shown in Fig. 7. $Mg_4Al_2TiO_{25}$ consists of nanocrystallites. Jayanthi et al. investigated the synthesis of $Mg_4Al_2TiO_{25}$ powder obtained by carbonated gel, which was cold pressed into green disks that were sintered at temperatures in the range of 1400–1600 °C (2–6 h) and cooled in a programmable electric furnace [2]. The grain size of $Mg_4Al_2TiO_{25}$ ranged from 40 μm to 80 μm with

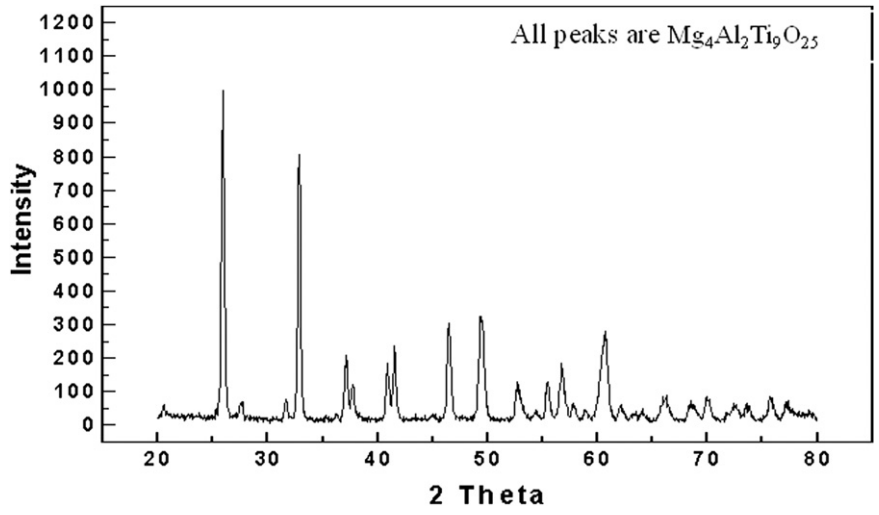

Fig. 5. X-ray diffraction pattern of the $Mg_4Al_2TiO_{25}$ compound sintered from $Al_2O_3+4MgO+9TiO_2$ powders.

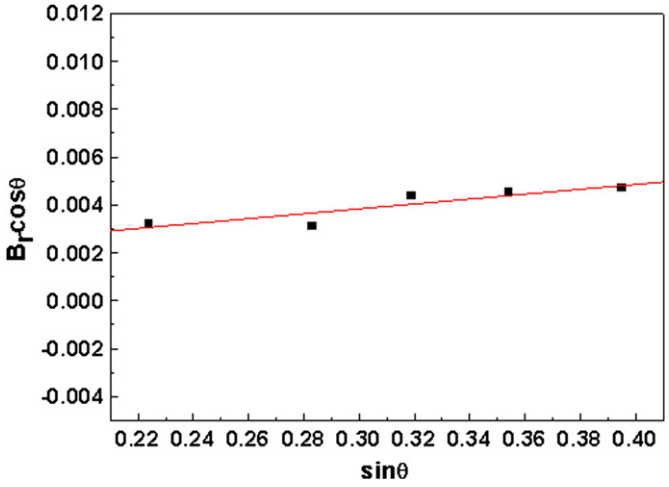

Fig. 6. Plot of B_r ($B_{crystalline}+B_{strain}$)cos θ versus sin θ for $Mg_4Al_2TiO_{25}$.

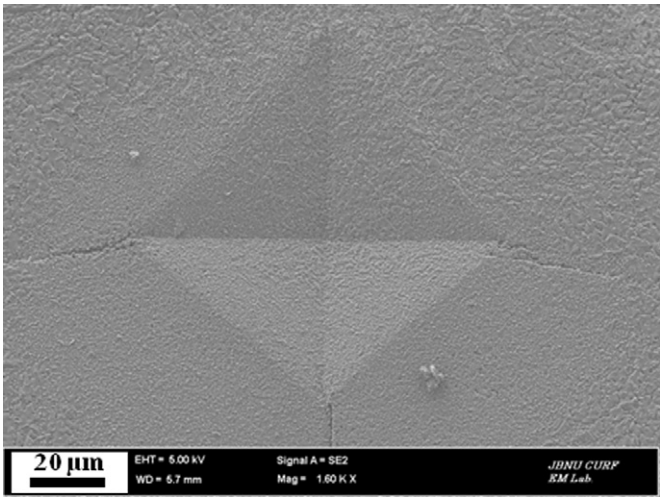

Fig. 8. Vickers indentations in the $Mg_4Al_2TiO_{25}$ compound sintered from milled powders.

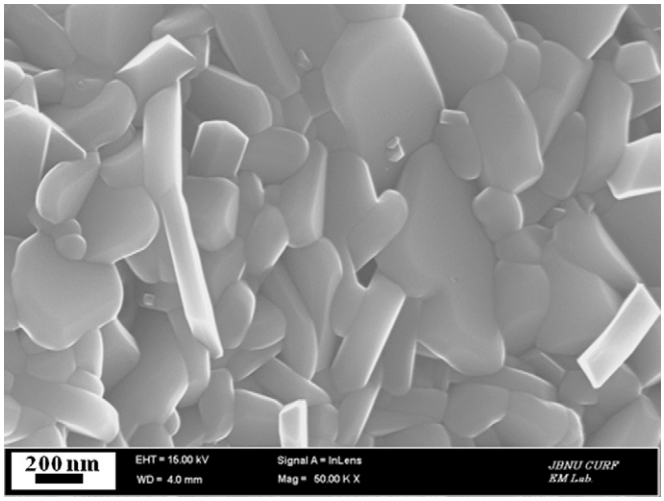

Fig. 7. FE-SEM image of the $Mg_4Al_2TiO_{25}$ compound sintered from $Al_2O_3+4MgO+9TiO_2$ powders.

a sintering temperature in the range of 1400–1600 °C. However, in this study the simultaneous synthesis and consolidation of $Mg_4Al_2TiO_{25}$ was accomplished from $Al_2O_3+4MgO+9TiO_2$ powders at a lower temperature within 1 min by one step, and nano-structured $Mg_4Al_2TiO_{25}$ was obtained.

The role of pulsed current in sintering or synthesis processes has been the focus of several attempts to provide an explanation for the observed enhancement of sintering and the improved characteristics of the products. The role played by the current has had various interpretations, with the effect explained in terms of a fast heating rate due to Joule heating, the presence of plasma in pores separating powder particles [14], and the intrinsic contribution of the current to mass transport [15–17].

Fig. 8 shows the Vickers indentations in the $Mg_4Al_2TiO_{25}$ compound sintered from $Al_2O_3+4MgO+9TiO_2$ powders.

Additional cracks (1–3) stemming from the indentation area were observed. The Vickers hardness of the $Mg_4Al_2TiO_{25}$ compound sintered from $Al_2O_3+4MgO+9TiO_2$ powders milled for 10 h was 780 kg/mm^2.

Indentations with sufficiently large loads produced median cracks near the indentation. The lengths of these cracks allow for the estimation of the fracture toughness of the materials [18]:

$$K_{IC} = 0.203(c/a)^{-3/2} H_v a^{1/2} \quad (3)$$

where c is the length of the crack measured from the center of the indentation, a is one-half of the average length of the two indent diagonals, and H_v is the hardness. The calculated fracture toughness for the $Mg_4Al_2TiO_{25}$ compound sintered from $Al_2O_3+4MgO+9TiO_2$ powders was 2.8 MPa m$^{1/2}$. The absence of reported values for the hardness and toughness on $Mg_4Al_2TiO_{25}$ prevents making direct comparisons to the results obtained in this work to show the influence of grain size.

4. Conclusions

Nanopowders of Al_2O_3, MgO and TiO_2 were made by high-energy ball milling. Using a PCAS rapid sintering method, the simultaneous synthesis and densification of nanostructured $Mg_4Al_2TiO_{25}$ compound was accomplished with $Al_2O_3+4MgO+9TiO_2$ powders within 1 min in one step. The Vickers hardness and fracture toughness of the $Mg_4Al_2TiO_{25}$ compound were 780 kg/mm^2 and 2.8 MPa m$^{1/2}$, respectively.

Acknowledgment

This work is partially supported by the KIST Future Resource Research Program and by the Human Resources Development of the Korea Institute of Energy Technology Evaluation and Planning (KETEP) grant funded by the Korea government Ministry of Knowledge Economy (No. 20114030200060).

References

[1] T.R.N. Kutty, P. Padmini, A method for the preparation of high purity lead titanate zirconate solid solutions by carbonate-gel composite powder precipitation, Journal of Materials Chemistry 7 (1997) 521–526.

[2] S. Jayanthi, T.R.N. Kutty, Microwave dielectric properties of $Mg_4Al_2Ti_9O_{25}$ ceramics, Materials Letters 62 (2008) 556–560.

[3] M. Sherif El-Eskandarany, Structure and properties of nanocrystalline TiC full-density bulk alloy consolidation from mechanically reacted powders, Journal of Alloys and Compounds 305 (2000) 225–238.

[4] L. Fu, L.H. Cao, Y.S. Fan, Two-step synthesis of nanostuctured tungsten carbide–cobalt powders, Scripta Materialia 44 (2001) 1061–1068.

[5] K. Niihara, A. Nikahira, Advanced Structural Inorganic Composite, Elsevier Scientific Publishing Co., Trieste, Italy, 1990.

[6] S. Berger, R. Porat, R. Rosen, Nanocrystalline materials: a study of WC-based hard metals, Progress in Materials Science 42 (1997) 311–320.

[7] I.J. Shon, K.I. Na, I.Y. Ko, J.M. Doh, J.K. Yoon, Effect of $FeAl_3$ on properties of (W,Ti)C–$FeAl_3$ hard materials consolidated by a pulsed current activated sintering method, Ceramics International 28 (2012) 5133–5138.

[8] A.I.Y. Tok, L.H. Luo, F.Y.C. Boey, Carbonate Co-precipitation of Gd_2O_3-doped CeO_2 solid solution nano-particles, Materials Science and Engineering A 383 (2004) 229–234.

[9] I.Y. Ko, N.R. Park, I.J. Shon, Fabrication of nanostructured $MoSi_2$–$TaSi_2$ composite by high-frequency induction heating and its mechanical properties, Korean Journal of Metals and Materials 50 (2012) 369–374.

[10] J. Jung, S. Kang, Sintered (Ti,W)C carbides, Scripta Materialia 56 (2007) 561–564.

[11] H.S. Kang, I.Y. Ko, J.K. Yoon, J.M. Doh, K.T. Hong, I.J. Shon, Properties and rapid low-temperature consolidation of nanocrystalline Fe–ZrO_2 composite by pulsed current activated sintering, Metals and Materials International 17 (2011) 57–62.

[12] I.J. Shon, H.Y. Song, S.W. Cho, W. Kim, C.Y. Suh, Mechanical synthesis and fabrication of nanostructured TiCo alloy by pulsed current activated sintering, Korean Journal of Metals and Materials 50 (2012) 39–44.

[13] C. Suryanarayana, M.Grant Norton, X-ray Diffraction a Practical Approach, Plenum Press, New York, 1998.

[14] Z. Shen, M. Johnsson, Z. Zhao, M. Nygren, Spark plasma sintering of alumina, Journal of the American Ceramic Society 85 (2002) 1921–1927.

[15] J.E. Garay, U. Anselmi-Tamburini, Z.A. Munir, S.C. Glade, P. Asoka- Kumar, Electric current enhanced defect mobility in Ni_3Ti intermetallic electric current enhanced defect mobility in Ni_3Ti intermetallics, Applied Physics Letters 85 (2004) 573–575.

[16] J.R. Friedman, J.E. Garay, U. Anselmi-Tamburini, Z.A. Munir, Modified interfacial reactions in Ag–Zn multilayers under the influence of high DC currents, Intermetallics 12 (2004) 589–597.

[17] J.E. Garay, J.E. Garay, U. Anselmi-Tamburini, Z.A. Munir, Enhanced growth of intermetallic phases in the Ni–Ti system by current effects, Acta Materialia 51 (2003) 4487–4495.

[18] K. Niihara, R. Morena, D.P.H. Hasselman, Evaluation of KIC of brittle solids by the indentation method with low crack-to-indent ratios, Journal of Materials Science Letters 1 (1982) 12–16.